

IRC–10443: A MULTI-PERIODIC SRa VARIABLE AND THE NATURE OF LONG SECONDARY PERIODS IN AGB STARSU. Munari¹ A. Siviero¹ P. Ochner² S. Dallaporta² C. Simoncelli²¹ *INAF Osservatorio Astronomico di Padova, via dell'Osservatorio 8, 36012 Asiago (VI), Italy*⁴ *ANS Collaboration, c/o Osservatorio Astronomico, via dell'Osservatorio 8, 36012 Asiago (VI), Italy*

Received 2008 August 30; revised September 3; accepted September 8

Abstract.

We obtained BVI_C photometry of IRC–10443 in 85 different nights distributed over two years, and in addition low resolution absolute spectrophotometry and high resolution Echelle spectroscopy. Our data show that IRC–10443, which was never studied before in any detail, is a SRa variable, characterized by $\Delta B=1.27$, $\Delta V=1.14$ and $\Delta I=0.70$ mag amplitudes and mean values $\langle B \rangle=13.75$, $\langle V \rangle=11.33$ and $\langle I_C \rangle=6.18$ mag. Two strong periodicities are simultaneously present: a principal one of $85.5 (\pm 0.2)$ days, and a secondary one of $620 (\pm 15)$ days, both sinusoidal in shape, and with semi-amplitudes $\Delta V=0.41$ and 0.20 mag, respectively. IRC–10443 turns out to be a M7III star, with a mean heliocentric radial velocity -28 km/s and reddened by $E_{B-V}=0.87$, a third of which of circumstellar origin. The same 0.5 kpc distance is derived from application of the appropriate period-luminosity relations to both the principal and the secondary periods. The long secondary period causes a sinusoidal variation in color of 0.13 mag semi-amplitude in $V - I_C$, with IRC–10443 being bluest at maximum and reddest at minimum, and with associated changes in effective temperature and radius of 85 K and 6% , respectively. This behavior of colors argues in favor of a pulsation nature for the still mysterious long secondary periods in AGB stars.

Key words: stars: pulsations – stars: variables – stars: AGB**1. INTRODUCTION**

IRC–10443 (= RAFGL 2209 = NSV 11129 = BD–12°5123) is a bright ($K=1.8$ mag) infrared source discovered during the Two Micron Sky Survey (Neugebauer and Leighton 1969), that lies in the general direction of the Scutum Star Cloud. IRC–10443 was detected by the AFGL survey (Price and Murdock 1983) at $4.2 \mu\text{m}$, and by IRAS satellite at 12 and $25 \mu\text{m}$. Its 2MASS magnitudes and colors are $K_s=1.92$, $J - H=1.35$, $J - K=1.80$. Its spectral type is reported to be M6 by Neckel (1958) and Hansen and Blanco (1975), and M6.5 by Nassau et al. (1956). IRC–10443 is present in the NSV catalog of suspected variables because I -band observations, obtained at five different epochs (from 21-08-1963 to 28-06-1965) which are reported in the IRC catalog, seem to trace a variation

from magnitude 6.4 to 6.9 (however, the uncertainty of the single measurement is similar to the dispersion of the five IRC measurements around their mean). Not much more is known about IRC–10443 and its nature. In this paper we report on our *BVI* photometric monitoring (85 nights distributed over two years) and optical spectroscopic observations (low and high resolution) of this object, and how they constrain its basic properties.

2. OBSERVATIONS

2.1. Photometry

BVI_C CCD photometry of IRC–10443 was independently obtained with two separate telescopes: (a) the 0.30-m Meade RCX-400 f/8 Schmidt-Cassegrain telescope owned by Associazione Astrofili Valle di Cembra (Trento, Italy). The CCD was a SBIG ST-9, 512×512 array, 20 μm pixels $\equiv 1.72''/\text{pix}$, with a field of view of $13' \times 13'$. The *B* filter was from Omega and the *VI_C* filters from Custom Scientific; and (b) the 0.50-m f/8 Ritchey-Cretien telescope operated on top of Mt. Zugna by Museo Civico di Rovereto (Trento, Italy) and equipped with Optec *BVI_C* filters. The CCD was an Apogee Alta U42 2048×2048 array, 13.5 μm pixels $\equiv 0.70''/\text{pix}$, with a field of view of $24' \times 24'$.

The comparison star for *B* and *V* bands was TYC 5699-6341-1, for which we adopted $B=11.016$ and $V=10.334$ in the standard Johnson *UBV* system. They were obtained from Tycho B_T, V_T data following Bessell (2000) transformations. The comparison star for *I_C* band was TYC 5699-6348-1 for which we adopted $I_C=6.39$, $V - I_C=0.55$ from the Hipparcos catalog. We had no alternatives for the comparison stars. In fact, these two are the only stars within the CCD field of view of IRC–10443 that (i) have reference magnitudes available in literature, (ii) are bright enough to be well exposed on the single CCD image without risking to saturate IRC–10443, and (iii) are photometrically stable to better than 0.02 mag. The last point was verified by noting that on all frames in any band we obtained, the relative magnitude of the two comparison stars was stable at this level.

All photometric measurements were corrected for instrumental color equations derived nightly by observations of Landolt (1992) standard fields. The good consistency of the data obtained independently with two different instruments reinforce our confidence in the accuracy of the results, in spite of the very red colors of IRC–10443, that are not reached by typical Landolt standard stars. Our photometry is presented in Table 1. It covers the period from 16-07-2006 to 11-07-2008, with observations collected in 85 different nights. The Poissonian component of the total error budget is less than 0.01 mag for all the data. The r.m.s. of the Landolt standard stars around the color equations they contributed to calibrate was on the average 0.019 mag for *B*, 0.022 for *V* and 0.031 for *I_C* bands.

2.2. Spectroscopy

A low resolution, absolutely fluxed spectrum of IRC–10443 was obtained on June 24.97, 2008 UT with the B&C spectrograph of INAF Astronomical Observatory of Padova attached to the 1.22m telescope operated in Asiago by the Department of Astronomy of the University of Padova. The slit, aligned with the parallactic angle, projected onto 2 arcsec on the sky, and the total exposure time was 1860 sec. The detector was an ANDOR iDus 440A CCD camera, equipped

Table 1. Our CCD photometry of IRC–10443. *a* and *b* identify the telescopes described in sect. 2.1.

| HJD | <i>B</i> | <i>V</i> | <i>I_C</i> | | HJD | <i>B</i> | <i>V</i> | <i>I_C</i> | |
|----------|----------|----------|----------------------|----------|----------|----------|----------|----------------------|----------|
| 3935.366 | 13.78 | 11.39 | 6.05 | <i>a</i> | 4289.557 | 13.74 | 11.29 | 6.22 | <i>b</i> |
| 3955.386 | 13.73 | 11.31 | 6.19 | <i>b</i> | 4296.517 | 13.65 | 11.20 | | <i>b</i> |
| 3966.387 | 13.75 | 11.42 | 6.24 | <i>a</i> | 4306.501 | | 11.17 | 6.17 | <i>b</i> |
| 3970.385 | 13.85 | 11.41 | 6.27 | <i>b</i> | 4309.340 | 13.50 | 11.15 | 6.16 | <i>b</i> |
| 3975.370 | 13.90 | 11.49 | 6.30 | <i>a</i> | 4312.369 | 13.60 | 11.20 | 6.17 | <i>b</i> |
| 3988.311 | 13.96 | 11.58 | 6.33 | <i>a</i> | 4314.423 | 13.70 | 11.22 | 6.15 | <i>b</i> |
| 4007.263 | 14.03 | 11.57 | 6.32 | <i>b</i> | 4316.435 | 13.73 | 11.25 | 6.18 | <i>b</i> |
| 4014.273 | 13.89 | 11.46 | 6.24 | <i>b</i> | 4351.345 | 14.12 | 11.64 | 6.30 | <i>b</i> |
| 4015.245 | 13.81 | 11.42 | 6.31 | <i>a</i> | 4356.371 | 14.08 | 11.60 | 6.22 | <i>b</i> |
| 4017.256 | 13.89 | 11.40 | 6.19 | <i>b</i> | 4358.350 | 14.05 | 11.52 | 6.22 | <i>b</i> |
| 4019.287 | 13.73 | 11.36 | 6.26 | <i>a</i> | 4360.318 | 13.99 | 11.50 | 6.20 | <i>b</i> |
| 4019.296 | 13.70 | 11.37 | 6.18 | <i>b</i> | 4363.319 | 13.90 | 11.45 | 6.18 | <i>b</i> |
| 4024.299 | 13.59 | 11.20 | 6.16 | <i>b</i> | 4374.334 | 13.65 | 11.21 | 6.09 | <i>b</i> |
| 4035.233 | 13.28 | 10.95 | 6.00 | <i>a</i> | 4376.325 | 13.58 | 11.17 | 6.05 | <i>b</i> |
| 4035.295 | 13.32 | 10.94 | 5.94 | <i>b</i> | 4381.316 | 13.55 | 11.13 | 6.01 | <i>b</i> |
| 4042.238 | 13.23 | 10.88 | 5.95 | <i>a</i> | 4386.328 | 13.64 | 11.16 | 6.06 | <i>b</i> |
| 4042.286 | 13.25 | 10.82 | 5.83 | <i>b</i> | 4389.143 | 13.67 | 11.21 | 6.10 | <i>b</i> |
| 4043.247 | 13.24 | 10.84 | 5.85 | <i>b</i> | 4392.309 | 13.69 | 11.24 | 6.10 | <i>b</i> |
| 4062.203 | 13.70 | 11.22 | 6.08 | <i>b</i> | 4405.243 | 13.97 | 11.50 | 6.25 | <i>b</i> |
| 4067.185 | 13.75 | 11.32 | 6.08 | <i>b</i> | 4406.269 | 13.95 | 11.50 | 6.30 | <i>b</i> |
| 4071.190 | 13.84 | 11.42 | 6.09 | <i>b</i> | 4417.208 | 14.24 | 11.81 | 6.41 | <i>b</i> |
| 4080.191 | | 11.50 | 6.16 | <i>b</i> | 4423.265 | 14.29 | 11.82 | | <i>b</i> |
| 4081.193 | | 11.51 | 6.22 | <i>b</i> | 4431.190 | 14.41 | 11.89 | 6.43 | <i>b</i> |
| 4151.717 | 13.71 | 11.43 | 6.18 | <i>b</i> | 4440.192 | 14.20 | 11.80 | 6.45 | <i>b</i> |
| 4158.690 | 14.04 | 11.62 | 6.45 | <i>b</i> | 4544.676 | 13.87 | 11.52 | 6.33 | <i>b</i> |
| 4168.660 | 14.05 | 11.63 | 6.39 | <i>b</i> | 4559.630 | 13.59 | 11.23 | 6.24 | <i>b</i> |
| 4174.657 | 14.00 | 11.59 | 6.36 | <i>b</i> | 4572.655 | 13.52 | 11.31 | 6.21 | <i>b</i> |
| 4181.629 | 13.96 | 11.50 | 6.28 | <i>b</i> | 4579.617 | 13.90 | 11.49 | 6.27 | <i>b</i> |
| 4193.576 | 13.70 | 11.24 | 6.13 | <i>b</i> | 4582.615 | 14.00 | 11.55 | 6.33 | <i>b</i> |
| 4196.595 | 13.61 | 11.17 | 6.13 | <i>b</i> | 4588.599 | 14.09 | 11.65 | 6.33 | <i>b</i> |
| 4196.644 | 13.59 | 11.16 | 6.08 | <i>a</i> | 4592.609 | 14.14 | 11.70 | 6.42 | <i>b</i> |
| 4201.585 | 13.40 | 10.96 | 6.01 | <i>b</i> | 4595.593 | 14.16 | 11.68 | 6.29 | <i>b</i> |
| 4201.652 | | 11.00 | 6.01 | <i>a</i> | 4598.594 | 14.13 | 11.66 | 6.28 | <i>b</i> |
| 4204.614 | 13.29 | 10.89 | 5.95 | <i>a</i> | 4600.596 | 14.06 | 11.68 | 6.32 | <i>b</i> |
| 4207.638 | 13.23 | 10.80 | 5.92 | <i>a</i> | 4614.534 | 13.72 | 11.43 | 6.30 | <i>b</i> |
| 4210.633 | | 10.80 | 5.96 | <i>b</i> | 4618.542 | 13.75 | 11.37 | 6.19 | <i>b</i> |
| 4211.635 | 13.14 | 10.75 | 5.88 | <i>a</i> | 4627.569 | 13.57 | 11.18 | 6.16 | <i>b</i> |
| 4218.634 | 13.21 | 10.83 | 5.92 | <i>a</i> | 4636.557 | 13.46 | 11.06 | 6.08 | <i>b</i> |
| 4229.609 | 13.65 | 11.14 | 6.09 | <i>a</i> | 4638.588 | 13.23 | 10.96 | 5.98 | <i>b</i> |
| 4231.588 | 13.74 | 11.23 | 6.08 | <i>b</i> | 4639.472 | 13.38 | 11.02 | 6.05 | <i>b</i> |
| 4239.586 | 13.92 | 11.43 | 6.25 | <i>b</i> | 4640.550 | 13.41 | 11.04 | 6.05 | <i>b</i> |
| 4239.590 | 14.03 | 11.42 | 6.22 | <i>a</i> | 4643.484 | 13.45 | 11.05 | 6.05 | <i>b</i> |
| 4260.579 | 14.18 | 11.82 | 6.45 | <i>a</i> | 4649.531 | 13.52 | 11.11 | 6.10 | <i>b</i> |
| 4275.512 | 14.16 | 11.70 | 6.35 | <i>b</i> | 4652.481 | 13.52 | 11.14 | | <i>b</i> |
| 4287.503 | 13.80 | 11.35 | 6.23 | <i>b</i> | 4658.500 | 13.66 | 11.25 | 6.20 | <i>b</i> |
| 4288.549 | 13.82 | 11.34 | 6.26 | <i>b</i> | | | | | |

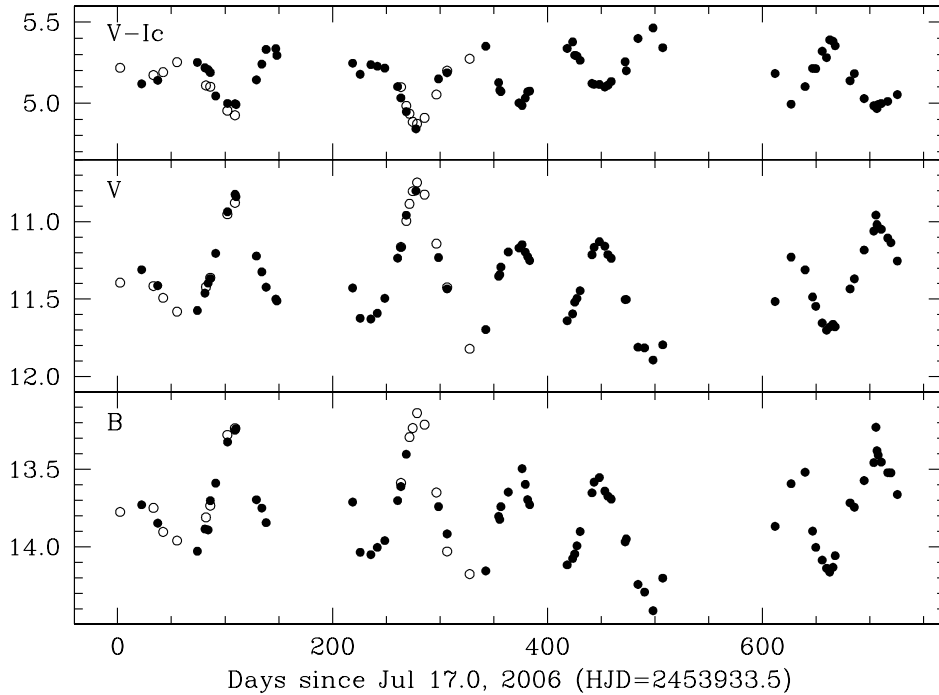


Fig. 1. Light- and color-curves of IRC 10443. Open circles: telescope *a*; filled dots: telescope *b* (see sect. 2.1).

with a EEV 42-10BU back illuminated chip, 2048×512 pixels of 13.5 μm size. A 300 ln/mm grating blazed at 5000 \AA provided a dispersion of 2.26 $\text{\AA}/\text{pix}$ and a covered range extending from 3250 to 7890 \AA .

High resolution spectra of IRC-10443 were obtained on June 10.04 and July 22.95 2008 UT with the Echelle spectrograph mounted on the 1.82m telescope operated in Asiago by INAF Astronomical Observatory of Padova. The detector was a EEV CCD47-10 CCD, 1024×1024 array, 13 μm pixel, covering the interval 3600–7300 \AA in 31 orders. A slit width of 200 μm provided a resolving power $R_P=26\,000$.

3. RESULTS

3.1. Photometric variability

The light-curve presented in Figure 1 clearly shows that IRC-10443 is indeed variable. The recorded variability amounts to $\Delta B=1.27$ (from 14.41 to 13.14), $\Delta V=1.14$ (from 11.89 to 10.75) and $\Delta I_C=0.70$ (from 6.45 to 5.75), around the mean values $\langle B \rangle=13.75$, $\langle V \rangle=11.33$ and $\langle I_C \rangle=6.18$ mag.

The variability is obviously periodic (see next section) and Figure 1 shows that the stars gets hotter (bluest $V - I_C$) at V maxima, and cooler (reddest $V - I_C$) at V minima. This behavior of the color is a distinctive features of stellar pulsation.

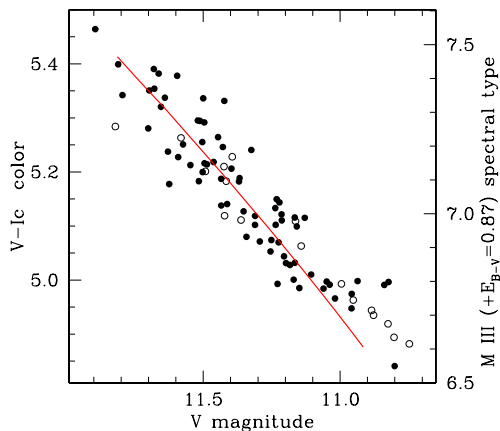


Fig. 2. Brightness-color diagram for the observations in Figure 1. The line is the path followed by a black-body, reddened by $E_{B-V}=0.87$, varying in radius and temperature at constant luminosity.

bands on the Fluks et al. (1994) spectra of M III giants reddened by $E_{B-V}=0.87$ (the amount affecting IRC-10443, see sect. 3.4)

IRC-10443 appears as a bona fide SRa variable. SRa variables are semi-regular late-type (M, C, S or Me, Ce, Se) giants displaying persistent periodicity and usually small ($\Delta V < 2.5$ mag) light amplitudes. Amplitudes and light-curve shapes generally vary and periods are in the range 35-1200 days. Many SRa differ from Miras only by showing smaller light amplitudes (Whitelock 1996).

3.2. Multi periodicities

Two main periodicities are at the same time present in IRC-10443: a principal and larger amplitude variation modulated by a 85.5 day period, and a secondary and smaller one of 620 days. The following expression corresponds to the curve fitting the V-band data in Figure 3 (where t is in HJD - 2450000):

$$V(t) = 11.38(\pm 0.02) + 0.41(\pm 0.02) \sin \frac{t - 4042.0(\pm 0.3)}{85.5(\pm 0.2)} + 0.22(\pm 0.02) \sin \frac{t - 4141(\pm 10)}{620(\pm 15)} \quad (1)$$

The combination of these two plain sinusoids provides a reasonably close fitting to the observed light-curve. Nevertheless, the residuals are larger than the observational errors, and an additional weaker component (either periodic or irregular) is probably present. Our present data are insufficient to characterize such an additional component, and to resolve it a much longer photometric monitoring is required, which we plan to pursue.

3.3. Spectral classification and radial velocity

The low resolution spectrum we obtained of IRC -10443 was compared with the digital spectral atlas of Fluks et al. (1994), that includes all spectral types from

In fact, Figure 2 plots the $V - I_C$ color against the V magnitude, showing the clear correlation between them. If we take a black-body, redden it by $E_{B-V}=0.87$, scale its flux so to match the average V band brightness of IRC-10443, and let it varies at constant luminosity, we obtain the line in Figure 2, which is a reasonably good fit to the observed points. This indicates that the variability displayed by IRC-10443 occurs at constant luminosity, in the form of expansion + cooling and contraction + warming, as expected in radial pulsations. The corresponding variation in spectral type goes from M6.6 III to M7.5 III as indicated on the right ordinate axis of Figure 2. These corresponding spectral types have been obtained by integrating the V and I_C

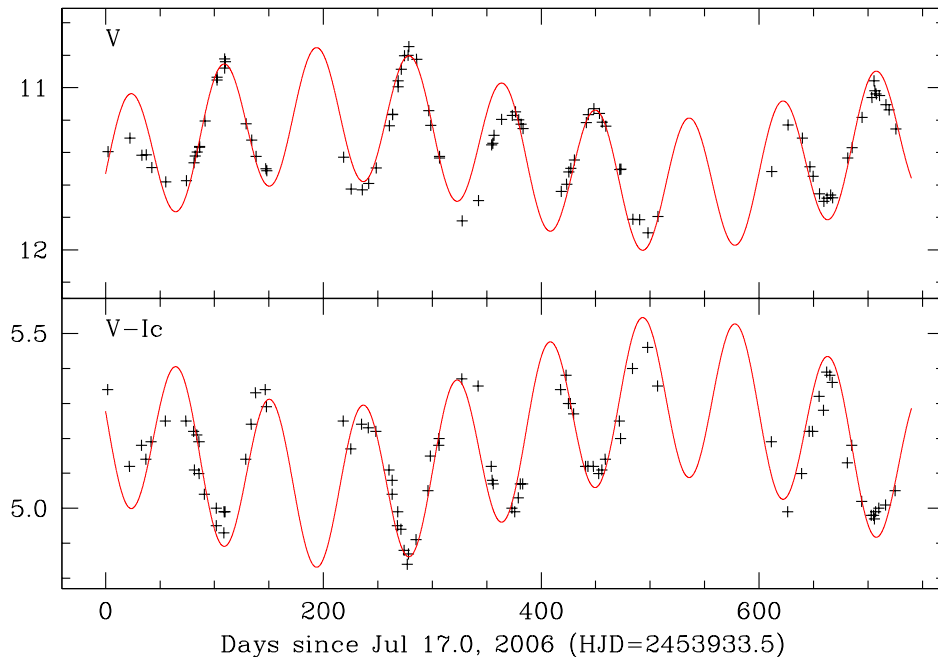


Fig. 3. Fitting of the V and $V - I_C$ light-curves of IRC-10443 with two sinusoids of 85.5 and 620 days periods (see sects. 3.2, 3.6 and Eq. 1).

M0 to M10 with spectra covering the whole optical range. They are of high flux accuracy and of a resolution similar to ours. Literature data suggest a M6/M6.5 spectral type for IRC-10443, but our spectrum is quite poorly fitted by the M6III reference spectrum from Fluks et al. (1994) library, while the match is perfect with a M7III spectrum, as shown in Figure 4. In view of the pulsation activity present in IRC-10443, the difference between our and other spectral classifications present in literature can be accounted for by the changes in surface temperature that characterize the pulsation activity (see right hand-side ordinates of Figure 2).

Figure 5 displays a portion centered on $H\alpha$ of our high resolution Echelle spectrum of IRC-10443 for July 22.95, and by comparison those of bracketing spectral types from the atlas of Bagnulo et al. (2003), degraded to the resolution of our Echelle spectrum via a Gaussian filter. The spectral progression in Figure 5 confirms the M7III classification for IRC-10443.

Mira variables displays emission lines, mainly the higher lines in the Balmer series, peaking in intensity at maximum brightness for both O- and C-rich varieties (e.g. Panchuk 1978, Yamashita et al. 1977, Mikulasek and Graf 2005), with large excursion in intensity along the pulsation cycle. When the first Echelle spectrum was exposed on June 10, IRC-10443 was on the rise and close to maximum brightness (pulsation phase 0.86), while for the July 22 spectrum it was declining and close to minimum brightness (pulsation phase 0.37). Both spectra do not show emission in the $H\alpha$ line, in agreement with the fact that the presence of emission lines is far less frequent in SR than in Mira variables.

The radial velocity of the M7III star is $-24.1(\pm 0.8)$ and $-31.4(\pm 0.7)$ km/s on the June 10 and July 22 spectra, respectively. The difference is well accounted

for by the pulsation activity. The two observations are separated in time by exactly half of the main 85.5 day pulsation period, and their mean value -28 km/s can be taken as representative of the systemic velocity of IRC-10443. At its galactic coordinates ($l=20^\circ$, $b=-3^\circ$) and distance (0.5 kpc, see below), the radial velocity expected from galactic disk rotation is $+7$ km/s (cf also Brand and Blitz 1993). The 35 km/s difference with the observed radial velocity, suggests that IRC-10443 does not belong to the young disk galactic population onto which it is seen projected and instead it is related to an older population. This is confirmed by the high tangential velocity, 86 km/s, derived from the proper motion listed in the NOMAD catalog (Zacharias et al. 2004) and the distance estimated in sect. 3.5 below.

3.4. Reddening

The fit with the Flucks et al. (1994) M7III reference spectrum presented in Figure 4 constrains the reddening affecting IRC-10443. The best match is obtained with $E_{B-V}=0.87\pm0.02$ for a standard $R_V=3.1$ reddening law.

The intrinsic $B - V$ color of M giants does not depend from the spectral type and hence the effective temperature, as illustrated by Johnson (1966), Lee (1970) and Fitzgerald (1970). Their tabular compilations provide $\langle(B - V)_0\rangle=+1.544$ as the mean intrinsic color of M5 to M8 class III giants. The mean $B - V$ color of our observations is $\langle(B - V)\rangle=+2.418$, which corresponds to a reddening $E_{B-V}=0.87\pm0.04$ affecting IRC 10443.

These two independent methods converge to the same amount of reddening affecting IRC 10443, $E_{B-V}=0.87\pm0.03$, which is adopted in this paper. A fraction of this total reddening is probably of circumstellar origin, as supported by the detection by Kwok et al. (1997) of emission from circumstellar dust in IRAS low resolution spectra. IRC-10443 lies in the general direction of the Scutum Star Cloud (SSC, centered at $l=27^\circ$, $b=-3^\circ$ galactic coordinates). SSC is one of the regions of the Milky Way with the highest stellar density, caused by unusually low extinction over its area. Reichen et al. (1990) presented the results of a detailed investigation of the extinction over the SSC based on ground-based and balloon-born UV survey data. Toward the direction to IRC-10443 they found that the interstellar reddening linearly increases with distance until $E_{B-V}\sim0.55$ is reached at 0.5 kpc. Longward, the further rise of the reddening with distance is very slow, reaching $E_{B-V}\sim0.65$ at 4 kpc. Only for distances $d>6$ kpc the reddening increases to $E_{B-V}\sim1$ (Madsen and Reynolds 2005).

Following the results of Reichen et al. (1990), we therefore conclude that $\sim1/3$ of the total $E_{B-V}=0.87$ reddening affecting IRC-10443, is of probable circumstellar origin.

3.5. Distance

In a seminal paper, Wood et al. (1999) used MACHO observations of late-type giant variables in LMC to produce a period-luminosity diagram for them, where five separate period-luminosity sequences were identified. Comparing with the model prediction of Wood and Sebo (1996), three of these sequences were found to coincide with the fundamental and first overtones pulsation modes, while the other two seemed to trace the variability induced by ellipsoidal distortion of RGB and AGB giants harbored in binary systems.

Since then, the availability of huge sets of data from large micro-lensing sur-

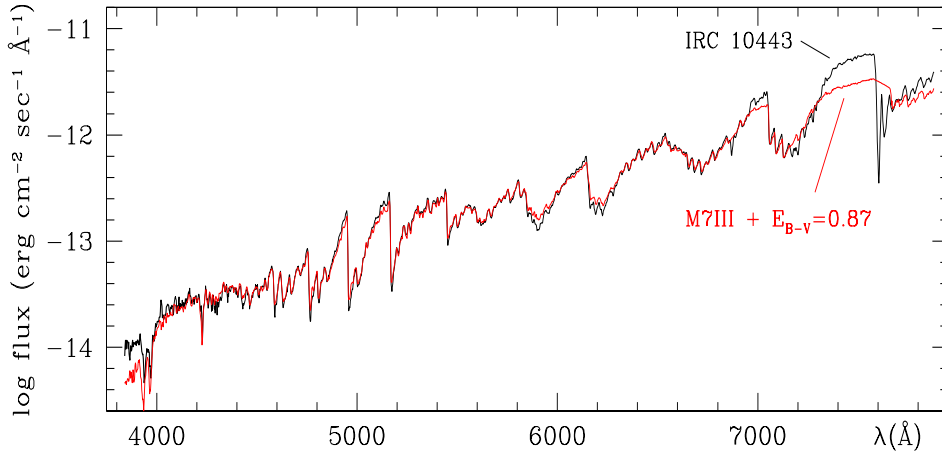


Fig. 4. Absolute spectro-photometry of IRC–10443 for 24.97 June 2008 UT (thick line) with superimposed the reference spectrum of a M7III star from the atlas of Fluks et al. (1994) reddened by $E_{B-V}=0.87$ (thin line).

veys (MACHO, OGLE, EROS, MOA) contributed to rapidly refine the picture, with now up to 14 different period-luminosity sequences identified (e.g. Kiss and Bedding 2003, Ita et al. 2004, Soszynski et al. 2005, Soszynski et al. 2007).

The most recent calibration of the various period-luminosity relations for late-type giant variables has been presented by Soszynski et al. (2007). Their relation for O-rich semi-regular variables of LMC takes the form $K_s = -4.35(\log P - 2.0) + 11.25$, where K_s band is that of the 2MASS survey. Whitelock et al. (2008) have shown that any chemical abundance effect on the K -band period-luminosity relation of Miras must be small. Working with the revised Hipparcos parallaxes of van Leeuwen (2007), Whitelock et al. (2008) have derived that period-luminosity relation of O-rich Miras in our Galaxy has the same slope and it is 0.1 mag brighter than the corresponding one for the LMC. We assume that a similar 0.1 mag shift would make the Soszynski et al. (2007) relations applicable to the O-rich SRA variables of our Galaxy. Adopting this 0.1 mag shift, a LMC distance modulus of $(m - M)_0 = 18.39$ (van Leeuwen et al. 2007), a LMC reddening of $E_{B-V} = 0.06$ (Mateo 1998), the extinction relation $A_{K_s} = 0.442E_{B-V}$ for an M-type spectral distribution and a standard $R_V = 3.1$ extinction law (Fiorucci and Munari 2003), the distance to IRC–10443 corresponding to the 85.5 day period is 0.5 kpc. Soszynski et al. (2007) relation for the long secondary periods of O-rich red giants in LMC takes the form $K_s = -4.41(\log P - 2.0) + 15.05$, and when applied (with the same 0.1 mag shift as above) to the 620 day secondary periodicity displayed by IRC–10443, it provides the same distance, 0.5 kpc, as obtained for the 85.5 day main period. Such 0.5 kpc distance is adopted for IRC–10443 in this paper.

3.6. On the nature of the long secondary period

In spite of large investigation efforts, both observational and theoretical, “the cause of the long secondary periods seen in cool giants remains a mystery at the present time” as recently remarked by Wood (2007).

It has been known for a long time that some semi-regular variables shows the presence of a long secondary period (LSP) in their light-curves, typically ten

times longer than the primary pulsation period. This ratio for IRC-10443 is 7.25. Lists of local giants displaying LSPs have been published, among others, by Houk (1963), Mattei et al. (1997), Kiss et al. (1999). Wood et al. (1999) found that $\sim 25\%$ of all variable AGB star in LMC show LSPs. A similar fraction, $\simeq 30\%$, of local semi-regular variables has been found by Percy et al. (2004) to display LSPs.

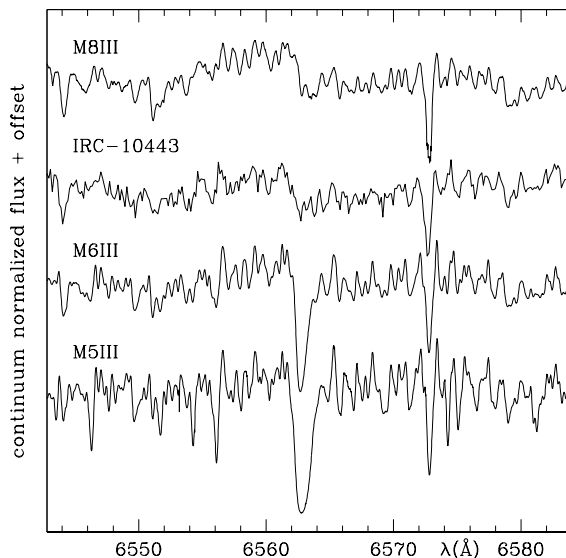


Fig. 5. Portion, centered on H α and CaI 6572.8, of the high resolution 22.95 July 2008 Echelle spectrum of IRC-10443. Spectra of cool giants from Bagnulo et al. (2003) are plotted for reference. All spectra are continuum normalized, offset in ordinates for better visibility, and shifted to 0.0 radial velocity.

The semi-regular variables appear to pulsate in the first overtone (Lebzelter and Wood 2006), and thus it could be tempting to relate the LSPs with pulsation in the fundamental mode. However, as found in theoretical models by Fox and Wood (1982) and verified by observations (e.g. Kiss et al. 1999, Mattei et al. 1997), the ratio of fundamental to first overtone periods is close to two, ruling out that LSPs are due to pulsations in the fundamental mode. Established observational facts are that LSPs are accompanied by radial velocity variations (of a lower amplitude than observed for the primary period; Hinkle et al. 2002, Wood et al. 2004) and by variation in intensity of the H α absorption (that could trace a variable filling by an emission component of chromospheric origin; Wood et al.

2004). In addition, cool variable giants showing LSPs rotate at similar velocity and show similar dust-free IRAS colors as cool variable giants not showing the LSPs (Olivier and Wood 2003). In RGB objects showing LSPs, the period of associated radial velocity variations is twice the period of photometric LSP variability (as expected in the case LSPs arise from ellipsoidally distorted giants in binary systems; Adams et al. 2006), while in AGB objects the period is the same (as expected in the case of pulsations; Wood et al. 2004). Various explanations of the LSP phenomenon have been proposed, but all have encountered some problems, as discussed by Wood (2007, and references therein).

A striking feature displayed by IRC-10443 is illustrated in the bottom panel of Figure 3, where the color variation is fitted with two sinusoids of the same periods of those fitting the V light-curve (cf Eq. 1 and the top-panel of Figure 3). Their semi-amplitudes are 0.23 mag for the sinusoid associated to the principal 85.5 day period, and 0.13 mag for the LSP, with a mean $V - I_C = 5.19$. From Figure 3, it is evident that IRC-10443 is bluest when it is at the maximum brightness along

the LSP cycle, and reddest when it is at the minimum brightness. This is the same pattern observed for the principal 85.5 day period and strongly argues in favor of a pulsation interpretation of LSP phenomenon, at least in IRC-10443. The simultaneous presence of two pulsations also accounts for the dispersion of the points in Figure 2 along the back-body curve. The dispersion would have been significantly reduced if only one pulsation would have been present, as confirmed by removing from observations one or the other of the sinusoidal variation of the color and re-plotting Figure 2.

The variation in $V - I_C$ color can be transformed into variation in effective temperature of the underlying stellar photosphere using the reference continuum energy distribution given by Fluks et al. (1994) along the spectral sequence of M giants. The total amplitude of 0.46 mag observed in $V - I_C$ for the principal period, corresponds to a change in 0.73 spectral types around the M7III mean, and therefore to a variation from 3030 to 3175 K in effective temperature. The 0.26 mag total color amplitude of the LSP would correspond to a change of 0.41 spectral types around the M7III mean, meaning a variation from 3060 to 3145 K. If both pulsations are supposed to occur at constant luminosity, the corresponding total excursion in radius is $\sim 10\%$ for the principal 85.5 day period, and $\sim 6\%$ for the LSP.

These excursions in radius are less than that inferred by Wood et al. (2004) from radial velocity observations at optical wavelengths of a sample of three hotter AGB stars characterized by longer LSP than IRC-10443. We estimated the change in *effective* temperature and radius of the underlying photosphere. If instead we had referred to a black-body fitting of the observed optical spectrum of the star (re-shaped by the extremely strong TiO molecular absorptions), the variation in *color* temperature and radius of IRC-10443 would have been almost twice larger, 150 K and 10 %, respectively.

It is worth noticing that recent theoretical improvements in the treatment of pulsation, like inclusion of time dependent turbulent convection (Olivier and Wood 2006), are opening new modeling possibilities for pulsation modes in cool giants. Important applications to the long lasting problem of what is driving the LSPs could be obtained in the near future (cf. Wood 2006). To better characterize the object and increase its interest as a test target for current theories, we plan to continue a tight observational monitoring of IRC-10443 over the next years, long enough to cover at least the whole next LSP period.

ACKNOWLEDGMENTS. We would like to thank P.A. Whitelock for useful comments on the original version of the paper, the anonymous referee for helpful suggestions, and S. Ciroi, F. Di Mille, S. Tomasoni, F. Moschini and M. Nave for assistance during the observations.

REFERENCES

- Adams E., Wood P. R., Cioni M. R. 2006, MSAIt 77, 537
 Bagnulo S., Jehin E., Ledoux C. et al. 2003, Messenger 114, 1

- Bessell M. S. 2000, *PASP* 112, 961
- Brand J., Blitz L. 1993, *A&A* 275, 67
- Fiorucci M., Munari U. 2003, *A&A* 401, 781
- Fitzgerald M. P. 1970, *A&A* 4, 234
- Fluks M. A., Plez B., The P. S. et al. 1994, *A&AS* 105, 311
- Fox M. W., Wood P. R. 1982, *ApJ* 259, 198
- Ita Y., Tanabe T., Matsunaga N. et al. 2004, *MNRAS* 353, 705
- Johnson H. L. 1966, *ARA&A* 4, 193
- Hansen O. L., Blanco V. M. 1975, *AJ* 80, 1011
- Hinkle K. H., Lebzelter T., Joyce R. R., Fekel F. C. 2002, *AJ* 123, 1002
- Houk N. 1963, *AJ* 68, 253
- Kiss L. L., Szatmry K., Cadmus R. R., Mattei J. A. 1999, *A&A* 346, 542
- Kiss L. L., Bedding, T. R. 2003, *MNRAS* 343, L79
- Kwok S., Volk K., Bidelman W. P. 1997, *ApJS* 112, 557
- Landolt A. U. 1992, *AJ* 104, 340
- Lebzelter T., Wood P. R. 2006, *MSAIt* 77, 55
- Lee T. A. 1970, *ApJ* 162, 217
- Madsen G. J., Reynolds R. J. 2005, *ApJ* 630, 925
- Mateo M. L. 1998, *ARA&A* 36, 435
- Mattei J. A., Foster G., Hurwitz L. A. et al. 1997, in *Hipparcos - Venice '97*, ESA SP-402, 269
- Mikulasek Z., Graf T. 2005, *CoSka* 35, 83
- Nassau J. J., Blanco V. M., Cameron D. M. 1956, *ApJ* 124, 522
- Neckel H. 1958, *ApJ* 128, 510
- Neugebauer G., Leighton R. B. 1969, *Two-Micron Sky Survey. A Preliminary Catalogue*, NASA SP, Washington
- Olivier E. A., Wood P. R. 2003, *ApJ* 584, 1035
- Olivier E. A., Wood P. R. 2006, *MSAIt* 77, 515
- Panchuk V. E. 1978, *SvAL* 4, 201
- Percy J. R., Bakos A. G., Besla G. et al. 2004, in *Variable Stars in the Local Group*, IAU Colloquium 193, D.W. Kurtz and K.R. Pollard eds., ASPC 310, 348
- Price S. D., Murdock T. L. 1983, *The Revised AFGL I.R. Sky Survey, Catalog and Supplement*, Air Force Geophysics Lab. AFGL-IR-83-0161
- Reichen M., Lanz T., Golay M., Huguenin D. 1990, *Ap&SS* 163, 275
- Soszynski I., Udalski A., Kubiak M. et al. 2005, *AcA* 55, 331
- Soszynski I., Dziembowski W. A., Udalski A. et al. 2007, *AcA* 57, 201
- van Leeuwen F. 2007, *Hipparcos: The New Reduction of the Raw Data*, Springer-Verlag
- van Leeuwen F., Feast M. W., Whitelock P. A., Laney C. D. 2007, *MNRAS* 379,

723

- Yamashita Y., Nariai K., Norimoto Y. 1977, An Atlas of Representative Stellar Spectra, Univ. of Tokyo Press
- Whitelock P. A. 1996, in Light Curves of Variable Stars, C.Sterken and C.Jaschek eds., Cambridge Univ. Press
- Whitelock P. A., Feast M. W., van Leeuwen F. 2008, MNRAS 386, 313
- Wood P. R., Sebo K. M. 1996, MNRAS 282, 958
- Wood P. R., Alcock C., Allsman R. A. et al. 1999, in Asymptotic Giant Branch Stars, T. Le Bertre, A. Lebre and C. Waelkens eds., IAU Symp 191, 151
- Wood P. R., Olivier E. A., Kawaler S. D. 2004, ApJ 604, 800
- Wood P. R. 2006, MSAIt 77, 76
- Wood P. R. 2007, in The 7th Pacific Rim Conference on Stellar Astrophysics, Y. W. Kang et al. eds., ASPC 362, 234
- Zacharias N., Monet D. G., Levine S. E. et al. 2004, AAS 205, 4815